

Supporting Information

Effective charge and energy transfer within a metal-organic framework for efficient photocatalytic oxidation of amines and sulfides

Shao-Dan Wang,[‡]^a Chun-Lin Lai,[‡]^a Yi-Xuan Zhang,^a Shu-Tong Bao,^a Kang-Le Lv^b and Li-Li Wen^{*a,c}

^a Key Laboratory of Pesticide & Chemical Biology of Ministry of Education, College of Chemistry, Central China Normal University, Wuhan, 430079, P. R. China.

^b Key Laboratory of Catalysis and Energy Materials Chemistry of Ministry of Education, South-Central University for Nationalities, Wuhan 430074, P. R. China.

^c State Key Laboratory of Structural Chemistry, Fujian Institute of Research on the Structure of Matter, Chinese Academy of Sciences, Fuzhou, Fujian 350002, P. R. China.

*Corresponding author. E-mail: wenlili@mail.ccnu.edu.cn (L. L. Wen)

[‡] Shao-Dan Wang and Chun-Lin Lai contributed equally to this work.

Experiment section

General procedures

All chemicals and solvents were commercially available and used as received. IR spectrum was recorded on a Bruker Tensor 27 spectrometer as dry KBr discs in the 400-4000 cm^{-1} region. All powder X-ray diffraction (PXRD) data were collected on a Bruker D8 Advance diffractometer using Cu-K α radiation ($\lambda = 1.5418 \text{ \AA}$) and 2θ ranging from 5 to 40° at room temperature. The UV-vis diffused reflectance spectra (DRS) were obtained on a Agilent Cary 100 UV-vis spectrophotometer with BaSO₄ as the reference for the baseline correction. The UV-vis spectrum for H₂O₂ Detection was collected on an Agilent Cary 60 spectrophotometer. Electron paramagnetic resonance (EPR) spectra were obtained on a Bruker EMXmicro EPR under visible-light irradiation. Scanning frequency: 9.83 GHz; central field: 3508.25 G; scanning power: 0.2 mW; scanning temperature: 25 °C. Room temperature photoluminescence (PL) emission spectra of the samples were collected on a FLS 1000 fluorescence spectrophotometer. Gas chromatography (GC) was recorded on GC-2010 Plus under the following conditions: oven temperature 280 °C, injector temperature 250 °C, column temperature program 10 °C/min, from 150 to 280 °C holding for 15 min. The light irradiation was obtained by a 6 W white LED. The electrochemical measurements were completed on a CHI760E electrochemical station in a standard three-electrode system with a graphite electrode (i.d. = 3 mm) as the working electrode system, a Pt electrode as the counter electrode, and an Ag/AgCl electrode as the reference electrode. Aqueous solution of Na₂SO₄ (0.5 M) was used as electrolyte.

X-ray crystallography

The crystallographic data for CCNU-16 was measured using a Bruker D8 Venture area-detector diffractometer with Ga-K α radiation ($\lambda = 1.34139 \text{ \AA}$) at 100 K. The structure was solved by direct methods and refined anisotropically with SHELXTL using full-matrix least-squares procedures based upon F^2 values [1]. In the structure, free solvent molecules were removed using the SQUEEZE routine of PLATON [2], the subsequent refinements were based on the new data generated. Crystallographic data has been deposited with the Cambridge Crystallographic Data Centre: CCDC 2116476. Select bond lengths and angles are provided in Table S2. In CCNU-16: Zn3A and Zn3B are disordered over two positions with site occupancy factors of 0.638(9)/0.362(9), O5A and O5B are similarly disordered with site occupancy factors of 0.638(9)/0.362(9) obtained by using SIMU and ISOR instructions. The part A was used to describe structure in the Diamond.

Synthesis of Zn-TPyP

The complex was synthesized via a modified procedure [3]. A mixture of 5,10,15,20-tetra(4-pyridyl)-21H,23H-porphine (H₂TPyP) (15 mg, 0.025 mmol), Zn(NO₃)₂·6H₂O (7.4 mg, 0.025 mmol), 3 mL of *N,N*-dimethylacetamide (DMA) and 0.1 mL HCl (0.1 M) were added to a 5 mL glass vial. After ultrasonication for 5 min, the mixture was sealed and heated at 100 °C for 48 h, and then cooled to room temperature. After washed with DMA and CH₃OH, purplish red crystals were collected in 40% yield based on H₂TPyP. IR (KBr, cm⁻¹): 3440s, 3088w, 1633s, 1593s, 1536m, 1464m, 1444m, 1364s, 1098w, 792m, 786m, 695w, 643m, 509w.

Recyclability of oxidative coupling of benzylamine over CCNU-16

After the reaction indicated above, the reaction solution was centrifuged at 8000 rpm for 1 min after each cycle and washed with *N,N*-dimethylformamide (DMF) and CH₃OH 3 times respectively. Then the catalyst was reused for the subsequent run with fresh benzylamine (0.4 mmol) under the optimized reaction conditions.

Recyclability of oxidation of thioanisole over CCNU-16

After the reaction indicated above, the reaction solution was centrifuged at 8000 rpm for 1 min after each cycle and washed with CH₃OH 3 times. Then the catalyst was reused for the subsequent run with fresh thioanisole (0.2 mmol) under the optimized reaction conditions.

H₂O₂ detection

Referring to the literature, *N,N*-diethyl-*p*-phenylenediamine (DPD)/horseradish peroxidase (POD) method was applied to investigate the generation of H₂O₂ [4]. Firstly, 10 μL of DPD was mixed in 10 mL of H₂SO₄ (0.05 M) solution and 10 mg of POD was dissolved in 10 mL of distilled water, both of which were stored at room temperature in dark. Then, the filtrate obtained after the photocatalytic oxidative coupling reaction of benzylamine over **CCNU-16** was added into 5 mL of H₂O, and the mixture was further extracted for three times to remove the organic compounds by ethyl acetate (EtOAc, 10 mL), and diluted to 100 mL with distilled water. Finally, by mixing 9 mL of above aqueous with 1 mL of PBS buffer (pH = 7.4) and using 3 mL of mixture as a test sample, after adding 3 mL of DPD and 3 mL of POD solution, the UV-Vis absorption spectrum of the sample was collected.

Electrochemical measurements

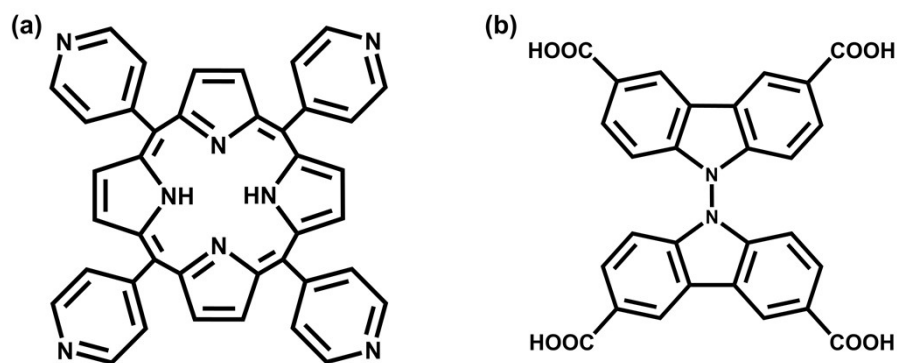
The catalyst (10 mg) was dispersed in 20 μL of 5 wt% Nafion and 1 mL of $\text{H}_2\text{O}/\text{CH}_3\text{OH}$ (v/v, 1:1) to obtain a suspension, and 20 μL of the suspension was scattered on the prepared graphite electrode then dried at room temperature in air. The Mott-Schottky plots were collected in 0.5 M Na_2SO_4 solution. The Mott-Schottky plots of **CCNU-16** were measured at frequencies of 500, 1000, and 1500 Hz. While the photocurrent signal measurement was performed with fluoride-tin oxide (FTO) glassy electrode (area of 0.8 cm^2) as the working electrode system under visible light from a 300 W xenon lamp with full spectrum.

Photoluminescence (PL) spectra

Typically, 3.0 mg **CCNU-16** (or 0.9 mg H_2TPyP , a fixed content of porphyrin) was dispersed in 6 mL DMF. Steady-state PL spectra were recorded under excitation at 420 nm and 520 nm.

Scavenger experiments

A series of photocatalyst-free radical scavengers were used to control the photoactivity experiments, i.e., KI and AgNO_3 were employed as the scavenger of photogenerated holes and electrons, *t*-butanol as the scavenger of hydroxyl radicals ($\cdot\text{OH}$), catalase as the scavenger of hydrogen peroxide (H_2O_2), 1,4-benzoquinone (BQ) as the scavenger of superoxide radical species ($\text{O}_2^{\cdot-}$), and 1,4-diazabicyclo[2.2.2]octane (DABCO) as the scavenger of singlet oxygen ($^1\text{O}_2$). Attempts were carried out similarly to the photocatalytic experiments where the radical scavengers (0.04 mmol or 5 μL of catalase) were added to the reaction system.



Scheme S1. Structures of H₂TPyP (a) and H₄BCTC (b).

Table S1. Crystallographic data and structure refinement for CCNU-16

CCNU-16	
Formula	C ₉₂ H ₅₄ N ₈ O ₁₉ Zn ₅
Formula weight	2006.46
Crystal system	orthorhombic
Space group	<i>Imma</i>
<i>a</i> /Å	28.4219(14)
<i>b</i> /Å	60.523(3)
<i>c</i> /Å	13.5431(6)
α /°	90
γ /°	90
β /°	90
<i>V</i> /Å ³	23297(2)
<i>Z</i>	4
ρ_{calcd} /g cm ⁻³	0.572
μ /mm ⁻¹	0.688
Collected reflections	108321
Unique reflections	12240
<i>R</i> ₁ [<i>I</i> > 2σ (<i>I</i>)]	0.0841
<i>wR</i> ₂ (all data)	0.3314
CCDC	2116476

Table S2. Selected bond distances (Å) and angles (deg) for CCNU-16

Zn1–O3#1	2.028(2)	Zn1–O3#2	2.028(2)
Zn1–O4	2.036(3)	Zn1–O4#3	2.036(3)
Zn1–O6	1.974(2)	Zn2–O1	2.237(17)
Zn2–O1#4	2.237(16)	Zn2–O2	2.080(3)
Zn2–O2#4	2.080(3)	Zn2–N2	2.079(2)
Zn2A–N2#4	2.079(2)	Zn3A–O5A	2.031(9)
Zn3A–N3	2.082(3)	Zn3A–N3#5	2.082(3)
Zn3A–N4	2.064(3)	Zn3A–N4#5	2.064(3)
O3#2–Zn1–O3#1	89.07(16)	O3#1–Zn1–O4#3	157.44(10)
O3#1–Zn1–O4	86.23(13)	O3#2–Zn1–O4#3	86.23(13)
O3#2–Zn1–O4	157.43(9)	O4#3–Zn1–O4	89.7(13)
O6–Zn1–O3#2	99.18(12)	O6–Zn1–O3#1	99.18(12)
O6–Zn1–O4	103.35(12)	O6–Zn1–O4#3	103.35(12)
O1#4–Zn2–O1	87.46(9)	O2–Zn2–O1	61.49(7)
O2#4–Zn2–O1	96.23(7)	O2–Zn2–O1#4	96.23(7)
O2#4–Zn2–O1#4	61.49(7)	O2–Zn2–O2#4	150.43(10)
N2#4–Zn2–O1#4	156.65(10)	N2–Zn2–O1#4	90.92(7)
N2#4–Zn2–O1	90.93(7)	N2–Zn2–O1	156.65(10)
N2#4–Zn2–O2#4	95.60(10)	N2–Zn2–O2#4	103.44(10)
N2#4–Zn2–O2	103.44(10)	N2–Zn2–O2	95.60(10)
N2–Zn2–N2#4	99.46(11)	O5A–Zn3A–N3	101.33(16)
O5A–Zn3A–N3#5	101.33(16)	O5A–Zn3A–N4#5	100.76(17)
O5A–Zn3A–N4#5	100.77(17)	N3#5–Zn3A–N3	157.3(3)
N4#5–Zn3A–N3#5	87.90(6)	N4–Zn3A–N3#5	87.90(6)
N4–Zn3A–N3#5	87.90(5)	N4–Zn3A–N3	87.90(6)
N4–Zn3A–N4#5	158.5(3)		

#1 1-x,1-y,1-z; #2 +x,1-y,1-z; #3 1-x,+y,+z; #4 1/2-x,+y,3/2-z; #5 -x,1/2-y,+z

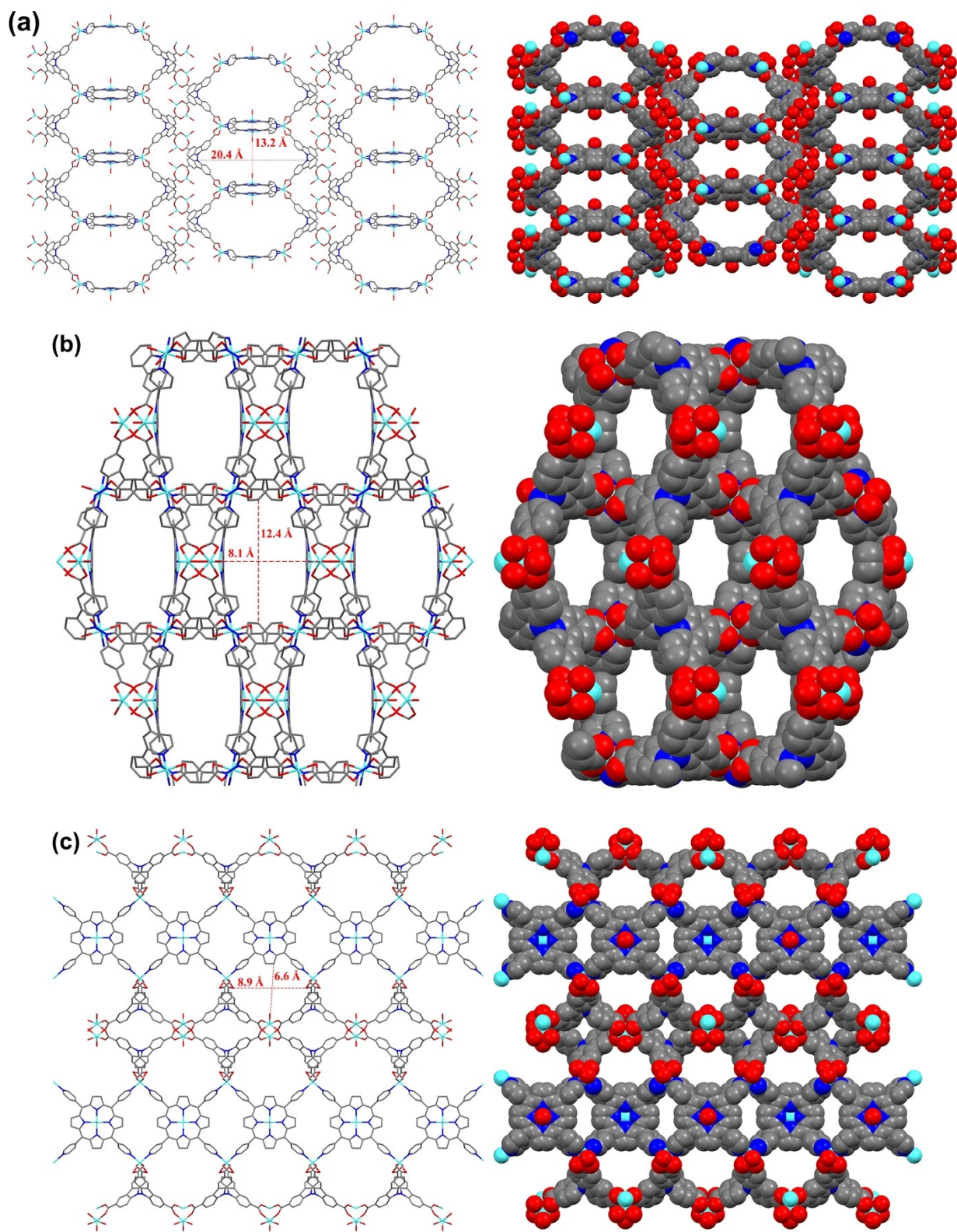


Fig. S1. (a) The space-filling structure along *a*-axis. (b) *b*-axis. (c) *c*-axis.

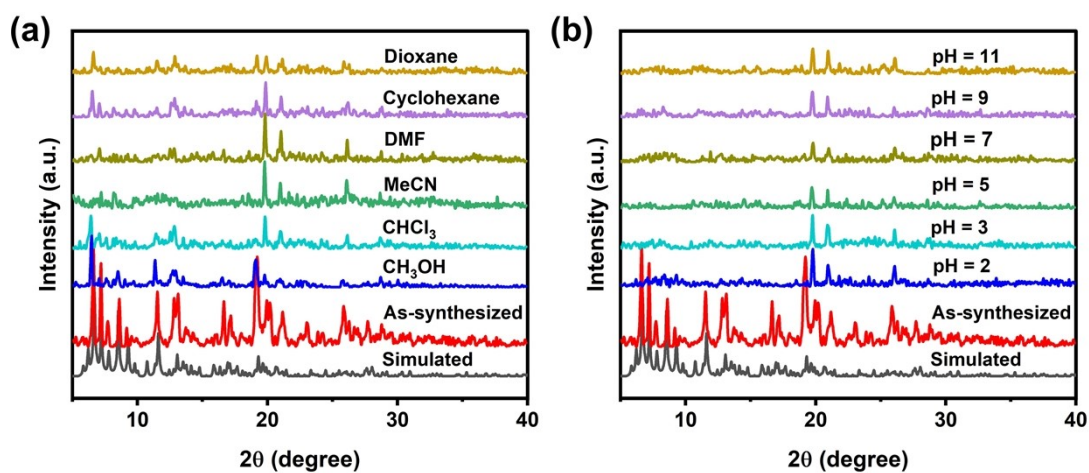


Fig. S2. PXRD patterns of CCNU-16 in organic solvents (a) and in aqueous solution with pH range of 2-11 (b) for 24 hours.

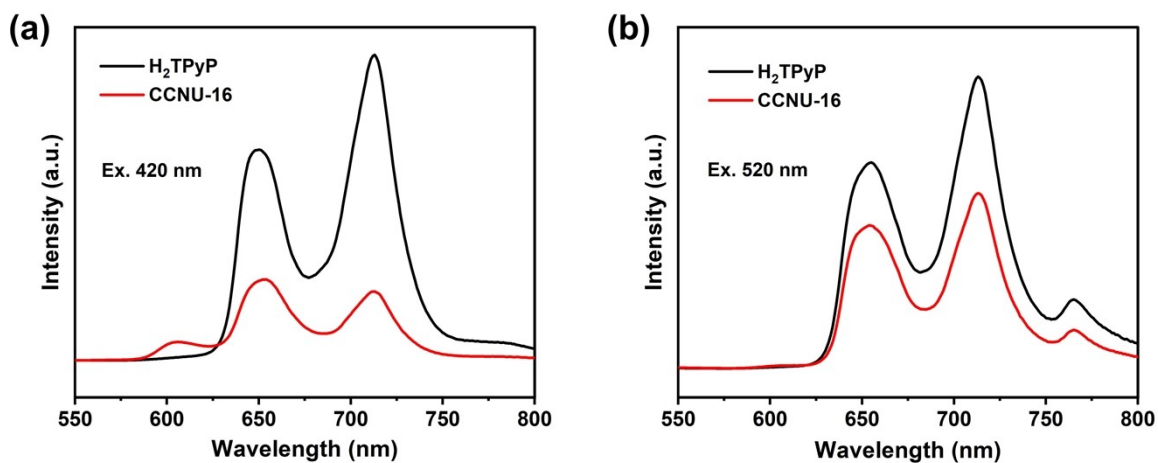


Fig. S3. Steady-state Photoluminescence (PL) spectra of H₂TPyP, Zn-TPyP and CCNU-16 under excitation at (a) 420 nm and (b) 520 nm, respectively.

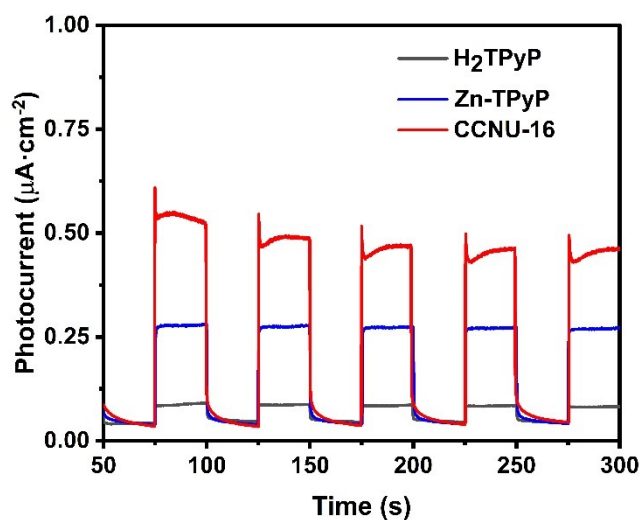
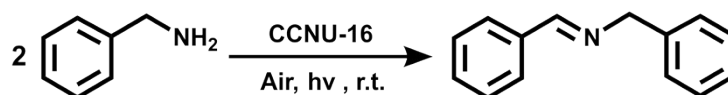


Fig. S4. Photocurrent response of H₂TPyP, Zn-TPyP and CCNU-16 with a fixed content of porphyrin unit under visible light (420 nm λ <math>< 800\text{ nm}</math>) irradiation.

Table S3. The solvent influence on the oxidative coupling of benzylamine over CCNU-16^a



Entry	Solvent	Conv. [%] ^b	Sel. [%] ^c
1	DMF	99	>99
2	DMA	95	>99
3	CH ₃ CN	76	>99
4	CH ₃ OH	34	>99
5	Cyclohexane	55	>99
6	Dioxane	66	>99

^a CCNU-16 (3.0 mg), benzylamine (0.4 mmol), solvent (1.0 mL), 6 W white LED, 65 min, air, 25.0 °C.

^b Determined by GC using toluene as the internal standard. ^c Determined by GC.

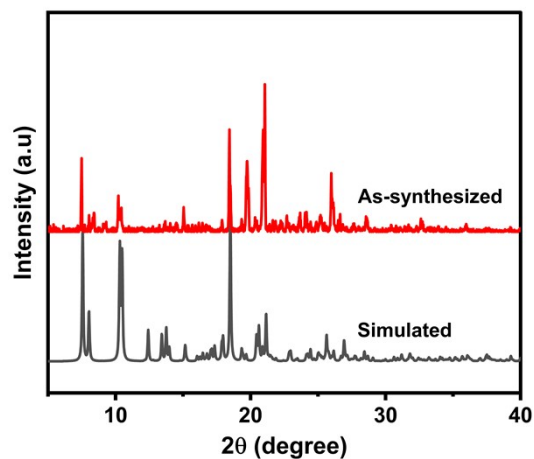


Fig. S5. XRD of Zn-TPyP synthesized via a modified procedure.

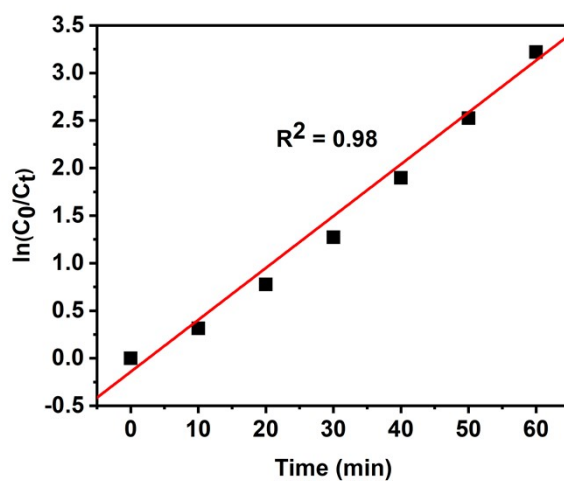


Fig. S6. Variation of $\ln(C_0/C_t)$ as a function of visible light irradiation time and linear fit of CCNU-16 photocatalyst. Reaction conditions: benzylamine (0.4 mmol), CCNU-16 (3.0 mg), DMF (1.0 mL), air, 6 W white LED. It could be seen that the plot of $\ln(C_0/C_t)$ against irradiation time generates a linear relationship ($R^2 = 0.98$), indicating that the photocatalytic oxidation benzylamine by CCNU-16 exhibits pseudo-first-order reaction kinetics.

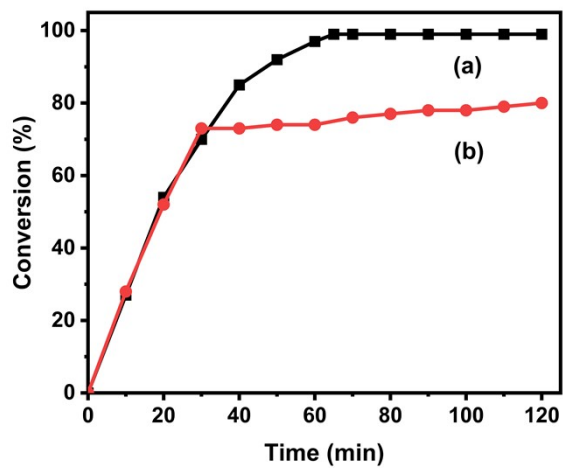
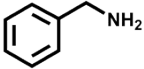
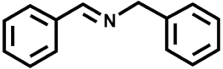
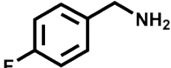
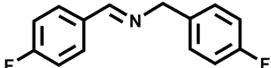
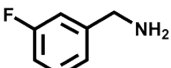
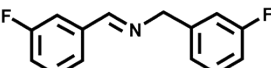
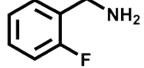
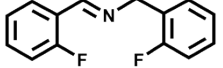
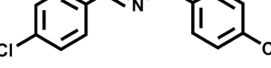
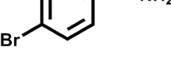
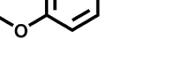
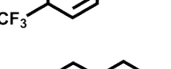
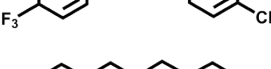
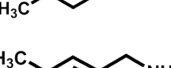
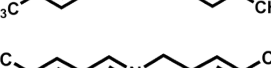
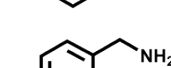
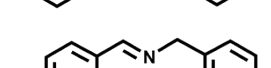
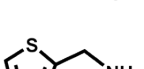
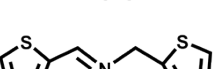
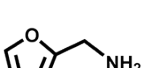
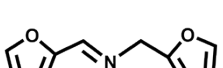
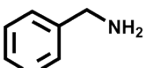
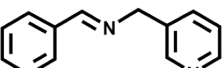
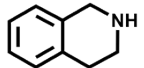
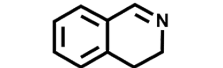
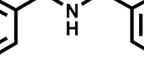
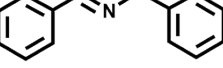
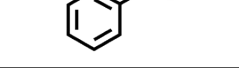
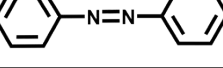
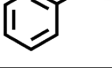
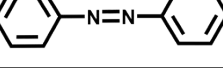


Fig. S7. Leaching test for the oxidative coupling of benzylamines over CCNU-16 under optimized reaction conditions. After 30 min of the reaction, the catalyst was filtered out whereas the filtrate was further reacted under identical conditions: (a) the common catalytic process and (b) hot filtration test.

Table S4. Aerobic photocatalytic oxidative coupling of various amines into imines by **CCNU-16^a**

Entry	Substrate	Product	Time [min]	Conv. [%] ^b	Sel. [%] ^c
1			65	99	99
2			65	99	99
3			75	99	99
4			85	99	99
5			75	99	99
6			75	99	99
7			65	99	99
8			85	99	99
9			65	99	99
10			75	99	99
11			95	99	99
12			120	99	99
13			100	99	99
14			105	99	99
15			85	99	99
16			70	99	99
17			130	—	—

^a CCNU-16 (3.0 mg), substrate (0.4 mmol), solvent (1.0 mL DMF), 6 W white LED, air, 25.0 °C. ^b Determined by GC using toluene as the internal standard. ^c Determined by GC.

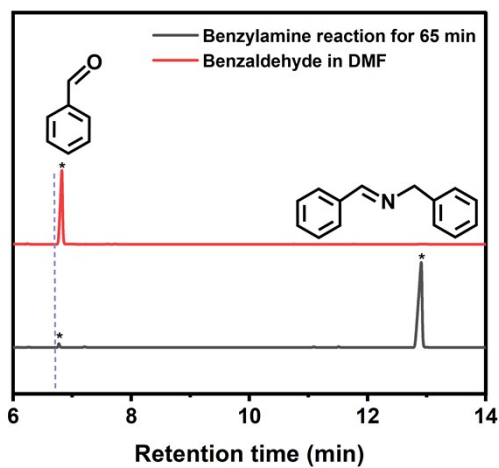


Fig. S8. Formation of trace amount of benzaldehyde after 65 min reaction of benzylamine.

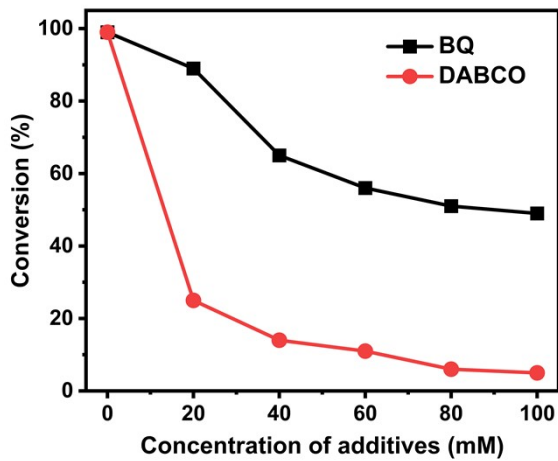
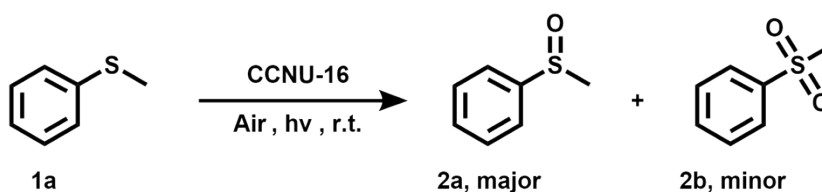


Fig. S9. Concentration influence of BQ (for $O_2^{\cdot-}$) and DABCO (for 1O_2) on benzylamine oxidative coupling over CCNU-16.

Table S5. The solvent influence on the oxidative coupling of thioanisole over CCNU-16^a



Entry	Solvent	Time [min]	Conv. [%] ^b	Sel. [%] ^c
1	CH ₃ OH	75	99	95
2	DMF	75	7	90
3	DMA	75	10	88
4	CH ₃ CN	75	38	94
5	Dioxane	75	50	92
6	CHCl ₃	75	18	97
7	CH ₃ OH:CH ₃ CN = 0.25:0.75	75	31	93
8	CH ₃ OH:CH ₃ CN = 0.5:0.5	75	48	98
9	CH ₃ OH:CH ₃ CN = 0.75:0.25	75	49	97
10	CH ₃ OH:CHCl ₃ = 0.25:0.75	40	88	97
11	CH ₃ OH:CHCl ₃ = 0.5:0.5	40	99	96
12	CH ₃ OH:CHCl ₃ = 0.75:0.25	40	99	95

^a CCNU-16 (3.0 mg), thioanisole (0.2 mmol), solvent (1.0 mL), 6 W white LED, air, 25.0 °C.

^b Determined by GC using toluene as the internal standard. ^c Determined by GC.

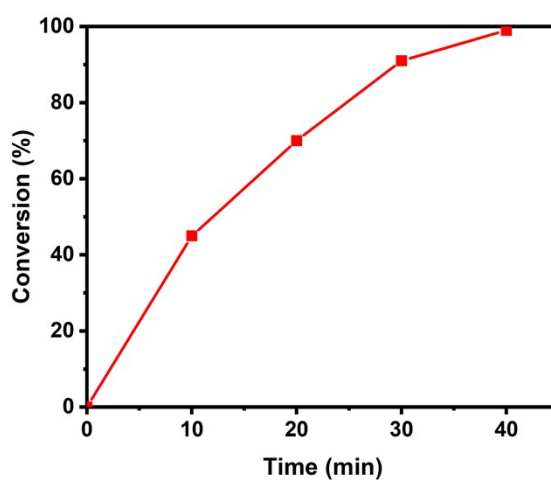


Fig. S10. The conversion of thioanisole with irradiation time over CCNU-16.

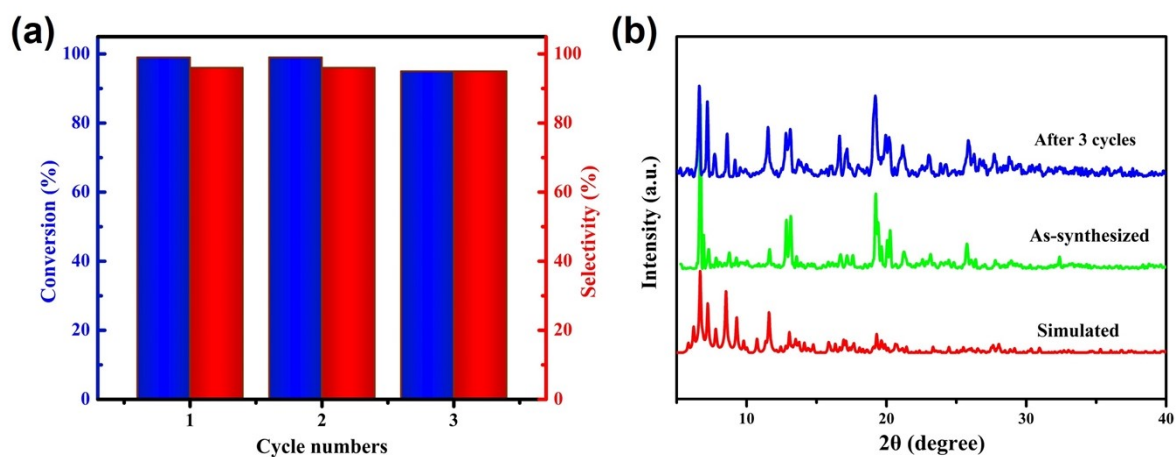


Fig. S11. (a) Cycling performance of CCNU-16 for the oxidation of thioanisole. (b) PXR D patterns for simulated CCNU-16 and experimental CCNU-16 before and after catalytic reaction.

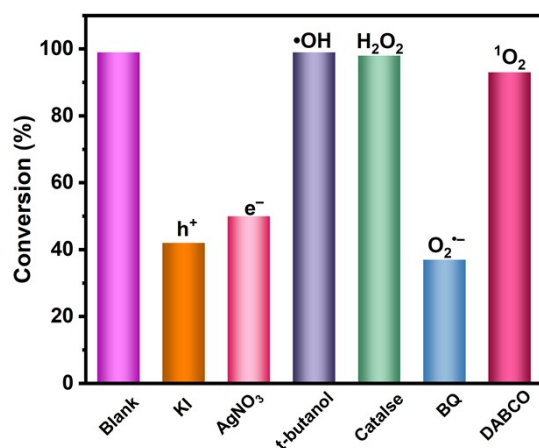


Fig. S12. Photocatalytic oxidation of thioanisole with the reactive species scavenger.

Table S6. Influence of BQ (for O₂^{•-}) and DABCO (for ¹O₂) on thioanisole oxidation over CCNU-**16^a**

Entry	Scavenger	n (mmol)	Conv. [%] ^b	Sel. [%] ^c
1	BQ	0.01	98	96
2	BQ	0.02	70	99
3	BQ	0.03	40	99
4	BQ	0.04	37	99
5	DABCO	0.01	99	89
6	DABCO	0.02	98	88
7	DABCO	0.03	94	89
8	DABCO	0.04	93	87

^a CCNU-**16** (3.0 mg), thioanisole (0.2 mmol), solvent (1.0 mL CH₃OH/CHCl₃ (1:1, v/v)), 6 W white LED, 40 min, air, 25.0 °C.^b Determined by GC using toluene as the internal standard.^c Determined by GC.

Table S7. Performances of visible-light-driven self-coupling of benzylamine using various photocatalysts

Entry	Photocatalyst	Light source	Oxidant	Time (h)	Conv. [%]	TOF (h ⁻¹) ^a	TOF (mmol g ⁻¹ h ⁻¹) ^b	Ref.
1	NH ₂ -MIL-125(Ti)	300 W Xe lamp (420-800 nm)	O ₂	12	73	5.3	—	5
2	UNLPPF-12	14 W CFL	Air	2	>99	67.5	—	6
3	Zn-PDI	500 W Xe lamp ($\lambda > 420$ nm)	Air	4	74	9.3	—	7
4	PCN-222	Xe lamp ($\lambda > 420$ nm), 100 mW/cm ²	Air	1	100	25.7	10	8
5	PCN-822(Hf)	LED light ($\lambda = 450$ nm), 100 mW/cm ²	1 atm O ₂	6	93	7.8	—	9
6	Cd(dcbpy)	300 W Xe lamp, UV-Vis	Air	7	99.1	1.2	3.4	10
7	NNU-45	300 W Xe lamp ($\lambda > 420$ nm)	O ₂ atmosphere	2.5	>99	13.4	—	11
8	[Zn ₃ (OH) ₂ (ADBE ₂) ₂] ₃ DEF	Visible light, 20.0 mW/cm ²	O ₂	1	99	45.8	—	12
9	ZJU-56-0.6	660 nm LEDs	O ₂ (60 °C)	24	84	3.5	—	13
10	Zn-bpydc	300 W Xe lamp	Air	4	99	—	6.2	14
11	FJI-Y10	300 W Xe lamp ($\lambda > 420$ nm)	O ₂ (40 °C)	6	100	4.2	—	15
12	Mn(ADBE ₂) ₂ (DMF) ₂	300 W Xe lamp (420 nm < λ < 800 nm)	O ₂ atmosphere	1	99	24.0	—	16
13	Pt/PCN-777	300 W Xenon lamp	N ₂	—	—	—	0.5	17

14	Ru(bpy) ₃ @MIL-125	Visible light ($\lambda > 440$ nm)	Air	3	75	—	2.5	18
15	CdS@MIL-101	300 W Xe lamp ($\lambda > 420$ nm)	Air (ice bath)	9	99	—	0.1	19
16	CdS@MOF-808	300 W Xe lamp ($\lambda > 400$ nm)	O ₂	1	95	—	9.5	20
17	CF-HCP	Green LED lamp (520 nm, 30 W)	1 atm O ₂	6	91	—	3.3	21
18	CoPz(hmdtn) ₄	$\lambda > 420$ nm visible light, 0.747 W/cm ²	1 atm O ₂	3	90	85.2	55.6	22
19	ZnP/CN	5 W LED lamp, 90 mW/cm ²	1 atm O ₂	1.5	99	—	115.0	23
20	2D-MoS ₂	White LED (400–700 nm, 45 W)	O ₂ (80°C)	72	99	—	0.2	24
21	WS ₂	White LED lamp (60 W)	O ₂ (50°C)	30	94	—	4.8	25
22	ZnS/CN	300 W Xe lamp ($\lambda > 400$ nm)	O ₂	5	92	—	0.9	26
23	TiO ₂ @N-C	Blue LEDs (450 nm, 3 W)	Air	15	95	—	0.7	27
24	CdS/Titanate	Green LED (520 nm, 3 W × 4)	Air	1.5	94	—	4.7	28
25	CCNU-16	6 W white LED	Air	1.08	99	121.0	60.3	This work

^a TOF = mmol product/(mmol catalyst × reaction time). ^b TOF = mmol product/(g catalyst × reaction time).

Table S8. Performances of visible-light-driven oxidation of thioanisole using various photocatalysts

Entry	Photocatalyst	Light source	Oxidant	Time (h)	Conv. [%]	Sel. [%]	TOF (h ⁻¹) ^a	TOF (mmol g ⁻¹ h ⁻¹) ^b	Ref.
1	[Zn ₂ (H ₂ O) ₄ Sn ^{IV} (TPyP)(HCOO) ₂] 4NO ₃ ·DMF·4H ₂ O	350 W Xe lamp	O ₂	12	>99.9	>99.9	0.8	—	29
2	UNLPF-10	Blue LED (135 mW, λ _{max} = 465 nm)	O ₂	8	99	99	104.0	—	30
3	[Zn(ADBEb)(DMA)]	300 W Xe lamp	O ₂	3.5	>99	>99	5.0	8.0	31
4	NNU-45	300 W Xe lamp (λ > 420 nm)	Air, H ₂ O ₂	4	99	95	16.7	23.5	11
5	Zr ₆ -Irphen	Blue light LED (100 W, λ = 460 nm)	O ₂	6	100	100	4.2	—	32
6	Zr-DTPP	25 W blue LED (5.0 mW/cm ² , 420 nm < λ _{em} < 490 nm)	O ₂	7	97	—	692.9	—	33
7	Zr ₁₂ -NBC	24 W blue LED light	Air	10	100	100	5.0	—	34
8	Ru ^{II} complex-based UIO-67	26 W fluorescent lamp	Air	22	72	—	16.6	—	35
9	3%-C ₆₀ @PCN-222	LED lamp (50 mW/cm ² , λ > 400 nm)	Air	3	> 99	100	80.0	3.3	36
10	3D-PdPor-COF	3 W blue LEDs	Air	0.4	98	—	49.0	—	37
11	<i>h</i> -LZU1	300 W Xe lamp (λ > 380 nm)	Air (30 °C)	22	100	92.6	—	1.3	38
12	DhaTph-Zn	300 W Xe lamp (λ > 400 nm)	1atm O ₂	10	82	>99	—	0.4	39

13	C ₃ N ₄ NSs-5 h	Xe lamp ($\lambda > 400$ nm)	0.1 MPa O ₂	1	99	99	—	50.0	40
14	TTO-COF	Blue LEDs (3 W \times 4)	0.1 MPa O ₂	2	90	98	—	26.5	41
15	P25 TiO ₂	300 W Xe lamp ($\lambda > 400$ nm)	O ₂	10	84	92	0.8	1.1	42
16	ARS-TiO ₂	300 W Xe lamp ($\lambda > 450$ nm)	O ₂	10	81	91	12.2	11.5	43
17	CdS/C ₃ N ₄	white LEDs (3 W \times 30, $\lambda > 420$ nm)	1 atm O ₂	6	61.8	99	—	6.1	44
18	ARS-Nb ₂ O ₅	Green LEDs (520 nm, 3 W \times 4)	Air	1.3	94	99	—	7.2	45
19	2-AA-TiO ₂	Violet LEDs (410 nm)	1 atm air	0.83	85	88	—	7.9	46
20	CCNU-16	6 W white LED	Air	0.67	99	96	190.7	95.0	This work

^a TOF = mmol product/(mmol catalyst \times reaction time). ^b TOF = mmol product/(g catalyst \times reaction time).

References

- [1] G. M. Sheldrick, *SHELXTL*, version 6.10, Bruker Analytical X-ray Systems; Madison, WI, 2001.
- [2] A.L. Spek, *J. Appl. Crystallogr.*, 2003, **36**, 7–13.
- [3] H. Krupitsky, Z. Stein, I. Goldberg and C.E. Strouse, *J. Incl. Phenom. Mol. Recogn. Chem.*, 1994, **18**, 177–192.
- [4] H. Bader, V. Sturzenegger and J. Hoignié, *Water Res.*, 1988, **22**, 1109–1115.
- [5] D. Sun, L. Ye and Z. Li, *Appl. Catal. B: Environ.*, 2015, **164**, 428–432.
- [6] J.A. Johnson, J. Luo, X. Zhang, Y.S. Chen, M.D. Morton, E. Echeverría, F.E. Torres and J. Zhang, *ACS Catal.*, 2015, **5**, 5283–5291.
- [7] L. Zeng, T. Liu, C. He, D. Shi, F. Zhang and C. Duan, *J. Am. Chem. Soc.*, 2016, **138**, 3958–3961.
- [8] C. Xu, H. Liu, D. Li, J.H. Su and H.L. Jiang, *Chem. Sci.*, 2018, **9**, 3152–3158.
- [9] Y. Zhang, J. Pang, J. Li, X. Yang, M. Feng, P. Cai and H.C. Zhou, *Chem. Sci.*, 2019, **10**, 8455–8460.
- [10] J. Shi, J. Zhang, T. Liang, D. Tan, X. Tan, Q. Wan, X. Cheng, B. Zhang, B. Han, L. Liu, F. Zhang and G. Chen, *ACS Appl. Mater. Interfaces*, 2019, **11**, 30953–30958.
- [11] H. Wei, Z. Guo, X. Liang, P. Chen, H. Liu and H. Xing, *ACS Appl. Mater. Interfaces*, 2019, **11**, 3016–3023.
- [12] P. Chen, Z. Guo, X. Liu, H. Lv, Y. Che, R. Bai, Y. Chi and H. Xing, *J. Mater. Chem. A*, 2019, **7**, 27074–27080.
- [13] H. Li, Y. Yang, C. He, L. Zeng and C. Duan, *ACS Catal.*, 2019, **9**, 422–430.
- [14] Y. Sha, J. Zhang, D. Tan, F. Zhang, X. Cheng, X. Tan, B. Zhang, B. Han, L. Zheng and J. Zhang, *Chem. Commun.*, 2020, **56**, 10754–10757.
- [15] F.J. Zhao, G. Zhang, Z. Ju, Y.X. Tan and D. Yuan, *Inorg. Chem.*, 2020, **59**, 3297–3303.
- [16] H. Liu, Z. Guo, H. Lv, X. Liu, Y. Che, Y. Mei, R. Bai, Y. Chi and H. Xing, *Inorg. Chem. Front.*, 2020, **7**, 1016–1025.

- [17] H. Liu, C. Xu, D. Li and H.L. Jiang, *Angew. Chem. Int. Ed.*, 2018, **57**, 5379–5383.
- [18] X. Yang, T. Huang, S. Gao and R. Cao, *J. Catal.*, 2019, **378**, 248–255.
- [19] R. Wu, S. Wang, Y. Zhou, J. Long, F. Dong and W. Zhang, *ACS Appl. Nano Mater.*, 2019, **2**, 6818–6827.
- [20] K. Gao, H. Li, Q. Meng, J. Wu and H. Hou, *ACS Appl. Mater. Interfaces*, 2021, **13**, 2779–2787.
- [21] Y. Zhi, K. Li, H. Xia, M. Xue, Y. Mu and X. Liu, *J. Mater. Chem. A*, 2017, **5**, 8697–8704.
- [22] J. Jin, C. Yang, B. Zhang and K. Deng, *J. Catal.*, 2018, **361**, 33–39.
- [23] W. Zou, X.L. Liu, C. Xue, X.T. Zhou, H.Y. Yu, P. Fan and H.B. Ji, *Appl. Catal. B: Environ.*, 2021, **285**, 119863.
- [24] Y. R. Girish, R. Biswas and M. De, *Chem. Eur. J.*, 2018, **24**, 13871–13878.
- [25] F. Raza, J. H. Park, H.-R. Lee, H.-I. Kim, S.-J. Jeon and Jong-Ho Kim, *ACS Catal.*, 2016, **6**, 2754–2759.
- [26] P. Chen, Li.-H. Meng, L. Chen, J.-K. Guo, S. Shen, C.-T. Au and S.-F. Yin, *ACS Sustainable Chem. Eng.*, 2019, **7**, 14203–14209.
- [27] F. Wang, X. He, L. Sun, L. Chen, X. Wang, J. Xu and X. Han, *J. Mater. Chem. A*, 2018, **6**, 2091–2099.
- [28] X. Dong, H. Hao, N. Wang, H. Yuan and X. Lang, *J. Colloid Interf. Sci.*, 2021, **590**, 87–395.
- [29] M.H. Xie, X.L. Yang, C. Zou and C.D. Wu, *Inorg. Chem.*, 2011, **50**, 5318–5320.
- [30] J.A. Johnson, X. Zhang, T.C. Reeson, Y.S. Chen and J. Zhang, *J. Am. Chem. Soc.*, 2014, **136**, 15881–15884.
- [31] X. Liang, Z. Guo, H. Wei, X. Liu, H. Lv and H. Xing, *Chem. Commun.*, 2018, **54**, 13002–13005.
- [32] L.Q. Wei and B.H. Ye, *ACS Appl. Mater. Interfaces*, 2019, **11**, 41448–41457.
- [33] X. Feng, X. Wang, H. Wang, H. Wu, Z. Liu, W. Zhou, Q. Lin and J. Jiang, *ACS Appl. Mater. Interfaces*, 2019, **11**, 45118–45125.
- [34] X.N. Zou, D. Zhang, T.X. Luan, Q. Li, L. Li, P.Z. Li and Y. Zhao, *ACS Appl. Mater. Interfaces*, 2021, **13**, 20137–20144.

- [35] C. Wang, Z. Xie, K.E. DeKrafft and W. Lin, *J. Am. Chem. Soc.*, 2011, **133**, 13445–13454.
- [36] D.Y. Zheng, E.X. Chen, C.R. Ye and X.C. Huang, *J. Mater. Chem. A*, 2019, **7**, 22084–22091.
- [37] Y. Meng, Y. Luo, J.L. Shi, H. Ding, X. Lang, W. Chen, A. Zheng, J. Sun and C. Wang, *Angew. Chem. Int. Ed.*, 2020, **132**, 3653–3658.
- [38] L. Liu, B. Zhang, X. Tan, D. Tan, X. Cheng, B. Han and J. Zhang, *Chem. Commun.*, 2020, **56**, 4567–4570.
- [39] Y. Qian, D. Li, Y. Han and H.L. Jiang, *J. Am. Chem. Soc.*, 2020, **142**, 20763–20771.
- [40] J. Li, Y. Chen, X. Yang, S. Gao and R. Cao, *J. Catal.*, 2020, **381**, 579–589.
- [41] F. Zhang, H. Hao, X. Dong, X. Li and X. Lang, *Appl. Catal. B: Environ.*, 2022, **305**, 121027.
- [42] X. Lang, W. Hao, W.R. Leow, S. Li, J. Zhao and X. Chen, *Chem. Sci.*, 2015, **6**, 5000–5005.
- [43] X. Lang, J. Zhao and X. Chen, *Angew. Chem. Int. Ed.*, 2016, **128**, 4775–4778.
- [44] Y. Xu, Z.C. Fu, S. Cao, Y. Chen and W.F. Fu, *Catal. Sci. Technol.*, 2017, **7**, 587–595.
- [45] X. Ma, H. Hao, W. Sheng, F. Huang and X. Lang, *J. Mater. Chem. A*, 2021, **9**, 2214–2222.
- [46] H. Li, X. Li, J. Zhou, W. Sheng and X. Lang, *Chin. Chem. Lett.*, 2022, **33**, 3733–3738.